Mass transport velocity in the ocean wave-driven free-surface boundary layer

S. Michele[a,b], **E. Renzi**[c], **A.G.L. Borthwick**[b], **T.S. van den Bremer**[d]
[a] Department of Civil Engineering and Computer Science, University of Rome Tor Vergata, Italy
[b] School of Engineering, Computing and Mathematics, University of Plymouth, UK
[c] Department of Mathematics, Physics and Electrical Engineering, Northumbria University, UK
[d] Faculty of Civil Engineering and Geosciences, Delft University of Technology, The Netherlands
michele@ing.uniroma2.it

Introduction

We present a mathematical model to investigate the mass transport velocity in the wave-driven free-surface boundary layer of the ocean under the influence of long crested progressive surface gravity waves. The continuity and momentum equations are solved within a Lagrangian framework. We assume that eddy viscosity is dependent on Lagrangian coordinates, and derive a new form of the second-order Lagrangian mass transport velocity, applicable across the entire finite water depth. Our results suggest the need to improve existing models that neglect the effects of free-surface boundary layer on ocean mass transport.

Governing equations

Consider two-dimensional water waves of amplitude A and frequency ω propagating at the top of a viscous fluid domain, where x is horizontal distance from a fixed origin, z is distance vertically upwards from the undisturbed free surface, and t is time. The fluid has constant depth h, and density ρ, whereas the eddy kinematic viscosity ν is assumed to be dependent on space and time. We further assume h to be comparable with the wavelength λ and much larger than the turbulent boundary layer thickness δ, so we expect the effects due to viscosity and turbulence to be localised in regions close to the free surface and seabed, whereas in the core region, the fluid motion is dominated by irrotational potential flow. Given that free-surface oscillations are much larger than δ, we use Lagrangian coordinates. Let a and b be the initial horizontal and vertical coordinates of a fluid particle, where $b = 0$ denotes the free surface and $b = -h$ the horizontal seabed. The continuity and momentum equations in Lagrangian form are given by [1]

$$[x,z] = \begin{vmatrix} \partial_a x & \partial_b x \\ \partial_a z & \partial_b z \end{vmatrix} = 1, \quad \rho\partial_{tt}x = -[P,z] + \rho\nu\nabla^2(\partial_t x) + 2\rho[\nu,z][\partial_t x,z] + \rho[x,\nu]([\partial_t z,z] + [x,\partial_t x]), \quad (1)$$

$$\rho\partial_{tt}z + g = -[x,P] + \rho\nu\nabla^2(\partial_t z) + 2\rho[x,\nu][x,\partial_t z] + \rho[\nu,z]([\partial_t z,z] + [x,\partial_t x]), \quad (2)$$

where (a,b) are fixed as the fluid particle moves from place to place, and the Lagrangian operator $\nabla^2 f = [[f,z],z] + [x,[x,f]]$. We assign zero stress at the free surface $b = 0$ and no motion at the horizontal seabed $b = -h$. The tangential and normal components of the stress tensor with respect to a material curve $(x(t), z(t))$ are

$$\boldsymbol{T_t} = \frac{\frac{\partial x}{\partial a}\frac{\partial z}{\partial a}(\tau_{zz} - \tau_{xx}) + \left[\left(\frac{\partial x}{\partial a}\right)^2 - \left(\frac{\partial z}{\partial a}\right)^2\right]\tau_{xz}}{|\boldsymbol{n}|^2}, \boldsymbol{T_n} = \frac{\left(\frac{\partial z}{\partial a}\right)^2\tau_{xx} + \left(\frac{\partial x}{\partial a}\right)^2\tau_{zz} - 2\frac{\partial x}{\partial a}\frac{\partial z}{\partial a}\tau_{xz} - \left[\left(\frac{\partial x}{\partial a}\right)^2 + \left(\frac{\partial z}{\partial a}\right)^2\right]P}{|\boldsymbol{n}|^2}, \quad (3)$$

where the normal and tangential vectors to the curve are given by $\boldsymbol{n} = (-\partial_a z, \partial_a x)$, $\boldsymbol{t} = (\partial_a x, \partial_a z)$, and the stress components in Lagrangian form read $\tau_{xx} = 2\nu\rho[\partial_t x, z]$, $\tau_{zz} = 2\nu\rho[x, \partial_t z]$ and $\tau_{xz} = \nu\rho([\partial_t z, z] - [\partial_t x, x])$. The Lagrangian velocity field can be found by adopting the perturbation expansion $\{x,z,P\} = \{a,b,-\rho g b\} + \{x_1,z_1,P_1\} + \{x_2,z_2,P_2\}$, where $\{x_1,z_1,P_1\} \sim O(\epsilon)$, $\{x_2,z_2,P_2\} \sim O(\epsilon^2)$, $\epsilon = Ak \ll 1$ represents small wave steepness and k is the wavenumber.

First-order solution

Solutions at first order are known for constant kinematic viscosity [2], whereas velocity components due to variable ν are not readily available. In what follows, we use a procedure based on boundary-layer theory to derive x_1, z_1. The free-surface displacement due to monochromatic regular waves of frequency ω and amplitude A is $\eta = \Re\{A\mathrm{e}^{\mathrm{i}(ka-\omega t)}\}$ where i denotes the imaginary unit. Let us also assume the following

decomposition $\{x_1, z_1\} = \{x_1^p + x_1^r, z_1^p + z_1^r\}$, where the superscript p denotes the irrotational (potential) component and r denotes the rotational part. We get

$$(\partial_t x_1^p, \partial_t z_1^p) = \nabla_L \Phi, \quad \nabla_L^2 \Phi = 0, \quad \rho \Phi_t = -P_1 - \rho g z_1, \quad \partial_a x_1^r + \partial_b z_1^r = 0, \tag{4}$$

$$\partial_{tt} x_1^r = \nu \nabla_L^2 \left(\partial_t x_1^r\right) + 2\partial_a \nu \partial_{ta} x_1^r + \nu_b \left(\partial_{ta} z_1^r + \partial_{tb} x_1^r\right), \partial_{tt} z_1^r = \nu \nabla_L^2 \left(\partial_t z_1^r\right) + 2\partial_b \nu \partial_{tb} z_1^r + \partial_a \nu \left(\partial_{ta} z_1^r + \partial_{tb} x_1^r\right), \tag{5}$$

where $\nabla_L = (\partial_a, \partial_b)$, Φ is the velocity potential for irrotational flow satisfying Laplace's equation, whereas the rotational components (x_1^r, z_1^r) are affected by fluid viscosity. Since $\delta \ll h$, the irrotational components x_1^p and z_1^p satisfy $\partial_b \Phi = 0$ at $b = -h$ and $\partial_b \Phi = \partial_t \eta$ at $b = 0$. Hence

$$x_1^p = \Re\left\{\mathrm{i}A \cosh[k(h+b)] \mathrm{e}^{\mathrm{i}(ka - \omega t)} / \sinh(kh)\right\}, \; z_1^p = \Re\left\{A \sinh[k(h+b)] \mathrm{e}^{\mathrm{i}(ka-\omega t)} / \sinh(kh)\right\}, \tag{6}$$

which correspond to the inviscid solution of monochromatic waves propagating over horizontal water depth h. The velocity components in the seabed boundary layer satisfy $x_1 = 0$ at $b = -h$ and $x_1 \to x_1^p$ as $(b+h)/\delta \to \infty$, which is now known. In this region the potential part and the kinematic viscosity ν do not change significantly, and we obtain the well-known solution [3]

$$x_1 = \Re\left\{\mathrm{i}A\left(1 - \mathrm{e}^{(\mathrm{i}-1)\frac{b+h}{\delta}}\right) \mathrm{e}^{\mathrm{i}(ka-\omega t)} / \sinh(kh)\right\}, z_1 = \Re\left\{\delta k A \left(\mathrm{e}^{(\mathrm{i}-1)\frac{b+h}{\delta}} - 1\right) \mathrm{e}^{\mathrm{i}(ka-\omega t)} / (1-\mathrm{i}) \sinh(kh)\right\}. \tag{7}$$

Similarly, in the free surface boundary layer the potential part remains almost constant and the hydrodynamics is dominated by viscous and turbulent effects. By assuming the boundary layer approximation, the x-momentum equation valid in the free-surface region subject to zero shear stress at $b = 0$, and matching with the outer flow (6) as $b/\delta \to -\infty$ gives

$$\partial_{tt} x_1^r = \partial_b \left(\nu \partial_{tb} x_1^r\right), \quad \partial_{tb} x_1^r = \Re\left\{-2\omega k A \mathrm{e}^{\mathrm{i}(ka-\omega t)}\right\} \; @ \; b = 0, \quad \partial_t x_1^r = 0 \; @ \; b/\delta \to -\infty. \tag{8}$$

The horizontal rotational velocity component can, in principle, be determined by solving (8) once ν has been prescribed. Many researchers have investigated the effects of depth-dependent eddy viscosity with the aim of deriving closed-form expressions for practical applications. Although the available models are relatively simplistic, they can approximate the averaged motion without the need for complex numerical simulations. Consequently, since we expect strong turbulence near the free surface, and based on the available studies, we adopt the following piece-wise eddy viscosity profile: $\nu = [\nu_s - b(\nu_m - \nu_s)/l] H[b+l] + \nu_m e^{\beta(b+l)} H[-b-l]$, where H denotes the Heaviside step function, ν_s is the eddy viscosity value at the free surface, and $\nu_m \geq \nu_s$ is the maximum eddy viscosity within the free-surface boundary layer. The location where $\nu = \nu_m$ is represented by $b = -l$, while β is a positive constant. In other words, we assume that the eddy viscosity initially increases linearly with depth, and for $b < -l$, it begins to decrease exponentially at a rate determined by the value of β because of decrease of turbulent effects. Solution of (8) is consequently given by

$$\begin{aligned} x_1^r = {} & \Re\left\{\left\{c_1 I_0\left[\frac{(1-\mathrm{i})\sqrt{l\omega\left[l\nu_s + b\left(\nu_s - \nu_m\right)\right]}}{\sqrt{2}(\nu_m - \nu_s)}\right] + c_2 K_0\left[\frac{(1-\mathrm{i})\sqrt{l\omega\left[l\nu_s + b\left(\nu_s - \nu_m\right)\right]}}{\sqrt{2}(\nu_m - \nu_s)}\right]\right\} \mathrm{e}^{\mathrm{i}(ka-\omega t)}\right\} H[b+l] \\ & + \Re\left\{c_3 e^{\frac{-a(b+l)}{2}} K_1\left[-\frac{2(-1)^{\frac{3}{4}} e^{-a\frac{b+l}{2}}}{a}\sqrt{\frac{\omega}{\nu_m}}\right] \mathrm{e}^{\mathrm{i}(ka-\omega t)}\right\} H[-b-l], \end{aligned} \tag{9}$$

where c_1, c_2 and c_3 are long complex constants not reported here for brevity, and I_n, K_n are the modified Bessel functions of first and second kind and of order n. The solution above can be significantly simplified if eddy viscosity is constant, i.e., $\nu = \nu_s = \nu_m$ and $\beta \to 0$. In this case we recover the well-known result [2] $x_1^r = \Re\{Ak(1-\mathrm{i})\delta \mathrm{e}^{\frac{(1-\mathrm{i})b}{\delta}} \mathrm{e}^{\mathrm{i}(ka-\omega t)}\}$, where $\delta = \sqrt{2\nu/\omega}$ is the viscous boundary layer thickness. The vertical velocity component z_1^r can be found by applying the continuity equation (4). Using boundary layer scales, we obtain $z_1^r \sim O\left(10^{-4}\right)$ m, which is taken to be negligible because of its very minor effect. The total first order solution in the free-surface boundary layer is finally given by $x_1 = \Re\left\{\mathrm{i}A \coth(kh) \mathrm{e}^{\mathrm{i}(ka-\omega t)}\right\} + x_1^r$, $z_1 = \Re\left\{A \mathrm{e}^{\mathrm{i}(ka-\omega t)}\right\}$. Using continuity of normal stress at $b = 0$ at order $O(Ak)$, we find $-P_1 + 2\rho\nu\partial_{tb} z_1 = 0$. Given that z_1 remains almost constant in the boundary layer, use of $P_1 = -\rho(\Phi_t + g z_1)$ gives $\omega^2 = gk \tanh(kh)$, hence higher-order wave-attenuation effects can be neglected.

Second-order solution

The horizontal and vertical momentum equations at second order for generalised eddy viscosity read

$$\rho\partial_{tt}x_2 = -\rho g\partial_a z_2 - \partial_a P_2 + \rho\nu\nabla_L^2\left(\partial_t x_2\right) + \rho\partial_a\nu\partial_{ta}x_2 + \rho\partial_b\nu\left(\partial_{tb}x_2 + \partial_{ta}z_2\right) + \rho\mathcal{G}, \tag{10}$$

$$\rho\partial_{tt}z_2 = -\rho g\partial_b z_2 - \partial_b P_2 + \rho\nu\nabla_L^2\left(\partial_t z_2\right) + \rho\partial_b\nu\partial_{tb}z_2 + \rho\partial_a\nu\left(\partial_{ta}z_2 + \partial_{tb}x_2\right) + \rho\mathcal{H}, \tag{11}$$

where the forcing terms $\mathcal{G}$ and $\mathcal{H}$ are given by quadratic products of first-order solutions [1]. The steady component $U_L = \overline{\partial x_2/\partial t}$ at second order is the mass transport velocity and is determined by time averaging over a wave period. By first integrating the time-averaged vertical momentum (11) and use the time-averaged inviscid condition at the free surface $\overline{P_2} = 0$ we get

$$\overline{z_2} + \frac{\overline{P_2}}{\rho g} - \overline{\eta_2} = -\int_c^0 \overline{\mathcal{H}} = \int_c^0 \frac{\omega^2 A k^2 \sinh[2k(b+h)]}{2\sinh^2(kh)}\,\mathrm{d}b, \tag{12}$$

where the overline denotes an averaged value, and $\mathcal{H}$ is dominated by the inviscid terms. In the latter equation, η_2 denotes the wave-setup and the right-hand side depends only on b because quadratic products are independent of a. Assuming $\nu = \nu(b)$, zero vertical flux, and substituting (12) into (10) we obtain the following equation for horizontal mass transport velocity in the free-surface boundary layer region

$$\partial_b\left(\partial_b U_L \nu\right) = 2A\omega k\coth\left(kh\right)\left[\Im\left\{\partial_b\left(\nu\partial_b x_1^r\right)\right\} + 2Ak\partial_b\nu\right]. \tag{13}$$

This can be integrated by applying a condition of zero stress $\partial_b U_L = 0$ at the free surface $b = 0$. After algebraic manipulation, we also get $\partial_b U_L \to 4A^2k^2\omega\coth\left(kh\right)$ at the outer edge of the free-surface boundary layer $b/\delta \to -\infty$; hence, Lagrangian mass transport outside the boundary layer is analogous to the case when the kinematic viscosity is constant [2]. By integrating (13), we obtain

$$U_L = U_{Li} + \frac{2Ak\omega}{\tanh(kh)}\Im\left\{x_1^r\right\} = \frac{A^2k\omega}{4}\left\{\frac{3 + 2\cosh[2k(b+h)]}{\sinh^2\left(kh\right)} + \frac{8k\left(h+b\right)}{\tanh(kh)}\right\} + \frac{2Ak\omega}{\tanh(kh)}\Im\left\{x_1^r\right\}, \tag{14}$$

where U_{Li} is the known inviscid solution. The expression above is new and includes the effects of spatial variations of $\nu(b)$ into x_1^r. We further note that U_L is always smaller than its inviscid approximation U_{Li}. In the simple case of constant eddy viscosity, we obtain the following explicit solution

$$U_L = \frac{A^2k\omega}{4}\left\{\frac{3 + 2\cosh[2k(b+h)]}{\sinh^2\left(kh\right)} + \frac{8k}{\tanh(kh)}\left\{h + b - \delta\mathrm{e}^{\frac{b}{\delta}}\left[\cos\left(\frac{b}{\delta}\right) + \sin\left(\frac{b}{\delta}\right)\right]\right\}\right\}, \tag{15}$$

which is also new and shows the decay due to the presence of the free-surface boundary layer.

Results

The effect of ocean turbulence can be included by considering simplified models based on constant eddy viscosity with values $\nu \sim O(10^{-2}) - O(10^{-3})\ \mathrm{m^2\ s^{-1}}$ much larger than the kinematic viscosity of water. Figure 1(a) shows the behaviour of the Lagrangian velocity U_L (14) with respect to the Lagrangian coordinate b for $\omega = 1.5\,\mathrm{rad\,s^{-1}}$ and constant eddy viscosity values $\nu_s = \nu_m = [10^{-4}; 10^{-3}; 10^{-2}]\,\mathrm{m^2\,s^{-1}}$. In the same figure, we also depict the inviscid approximation U_{Li}, represented by a black curve. We observe that the inviscid approximation is characterised by the highest velocity at the free surface, whereas for $b < \delta$, each profile quickly approaches U_{Li}. We now examine the impact of various eddy viscosity profiles on the behaviour of U_L for $\omega = 1.5\,\mathrm{rad\,s^{-1}}$ and $\nu_m = 10^{-2}$ ($\mathrm{m^2\ s^{-1}}$). Table 1 provides a summary of the nine profiles considered, where $\delta_m = \sqrt{2\nu_m/\omega}$. Profile 1 corresponds to the case of constant eddy viscosity. Profiles 2 to 5 are characterised by an exponential decay starting from $b = -\delta_m/2$, whereas the decay of eddy viscosity in Profiles 6 to 9 occurs at a deeper value $b = -3\delta_m$. Profiles 3, 5, 7, and 9 are characterised by a linear increase in eddy viscosity from the free surface, whereas the remainder exhibit a constant value before the decay begins. Finally, the different values of $\beta = [4.88, 48.8]\,\mathrm{m^{-1}}$ determine the slow or rapid exponential decay in $b < -l$, respectively. Figure 1(b) illustrates the Lagrangian mass transport velocity U_L for each of the nine profiles along with the inviscid approximation U_{Li}. We immediately note that the

Profile	ν_s	β	l/δ_m	Profile	ν_s	β	l/δ_m	Profile	ν_s	β	l/δ_m
1	10^{-2}	0	∞	4	10^{-2}	48.8	0.5	7	10^{-3}	4.88	3
2	10^{-2}	4.88	0.5	5	10^{-3}	48.8	0.5	8	10^{-2}	48.8	3
3	10^{-3}	4.88	0.5	6	10^{-2}	4.88	3	9	10^{-3}	48.8	3

Table 1: Parameters describing the nine eddy viscosity profiles.

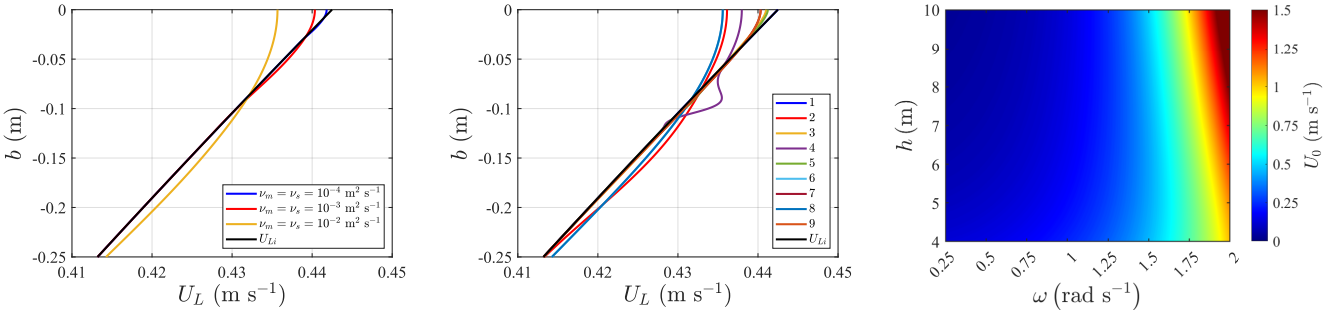

Figure 1: (a): Lagrangian mass transport velocity U_L versus b for $A = 0.5$ m, $h = 5$ m, $\omega = 1.5$ rad s^{-1} and constant viscosity $\nu_s = \nu_m = [0; 10^{-4}; 10^{-3}; 10^{-2}]$ m^2 s^{-1}. The black line represents the inviscid approximation U_{Li}. (b) U_L versus b for $A = 0.5$ m, $h = 5$ m, $\omega = 1.5$ rad s^{-1} for the eddy viscosity profiles. (c): U_0 versus h, ω and fixed $A = 0.5$ m, $\nu_s = \nu_m = 10^{-2}$ m^2 s^{-1}.

constant Profile 1 exhibits the smallest value of U_0 whereas U_{Li} has the greatest mass transport velocity value at the free-surface. Profile 2 features constant eddy viscosity up to $b = -\delta_m/2$, beyond which it decays exponentially. Here, the velocity profile resembles that of Profile 1, though with a slightly higher value in the range $-l < b < 0$. For $b \ll -l$, the profile mirrors the behaviour of U_{Li} due to the exponential decay of ν. Profiles 3, 5, 7 and 9, all characterized by the smallest ν_s, yield velocity profiles that closely align with the inviscid approximation. This indicates that when the free-surface eddy viscosity ν_s is small, the Lagrangian mass transport velocity can be approximated as $U_L \sim U_{Li}$ with good accuracy. The main difference occurs in a region close to the free-surface, where viscosity effects are dominant. Specifically, Profiles 7 and 9 allow greater mass transport velocity because of slower increase in ν with depth. Also, we note that the exponential decay does not have a significant effect. Profile 4 represents a profile that has constant eddy viscosity in the range $-\delta_m/2 < b < 0$, and a rapid (exponential) decrease in ν for $b < -\delta_m/2$. In particular, the corresponding mass transport velocity has a bump in the region close to $b = -l$ and then quickly approaches U_{Li} due to a rapid exponential decay in ν. Curves for Profiles 6 and 8 are practically coincident with that for Profile 1. This is due to the constant value of ν in the range $-3\delta_m < b < 0$ and the exponential decay of eddy viscosity occurring outside the boundary layer thickness δ_m. Figure 1(c) shows the mass transport velocity at the free surface U_0 versus ω and h for constant eddy viscosity $\nu_s = \nu_m = 10^{-2}$ m^2 s^{-1}. The velocity U_0 increases with ω as also shown by (15). Furthermore, U_0 increases or decreases with water depth h depending on whether the value of wave frequency is greater or smaller than $\omega \sim 1.5$ rad s^{-1}, underlining the importance of the new finite-depth results we have derived.

REFERENCES

[1] Michele, S., Renzi, E., Borthwick, A., and van den Bremer, T. 2025. *Heat transfer and mass transport in the ocean wave-driven free-surface boundary layer. J. Fluid Mech. 1010*, A7.

[2] Ünlüata, U., and Mei, C. C. 1970. *Mass transport in water waves. J. Geophys. Res. 75*, 7611–7618.

[3] Longuet-Higgins, M. S. 1953. *Mass Transport in Water Waves. Philos. Trans. R. Soc. 345*, 535–581.